Contrib Mineral Petrol (1998) 133: 169–185

Mihai N. Ducea · Jason B. Saleeby

The age and origin of a thick mafic–ultramafic keel from beneath the Sierra Nevada batholith

Received: 27 December 1997 / Accepted: 11 June 1998

Abstract We present evidence for a thick (~100 km) sequence of cogenetic rocks which make up the root of the Sierra Nevada batholith of California. The Sierran magmatism produced tonalitic and granodioritic magmas which reside in the Sierra Nevada upper- to mid-crust, as well as deep eclogite facies crust/upper mantle mafic–ultramafic cumulates. Samples of the mafic–ultramafic sequence are preserved as xenoliths in Miocene volcanic rocks which erupted through the central part of the batholith. We have performed Rb-Sr and Sm-Nd mineral geochronologic analyses on seven fresh, cumulate textured, olivine-free mafic–ultramafic xenoliths with large grainsize, one garnet peridotite, and one high pressure metasedimentary rock. The garnet peridotite, which equilibrated at ~130 km beneath the batholith, yields a Miocene (10 Ma) Nd age, indicating that in this sample, the Nd isotopes were maintained in equilibrium up to the time of entrainment. All other samples equilibrated between ~35 and 100 km beneath the batholith and yield Sm-Nd mineral ages between 80 and 120 Ma, broadly coincident with the previously established period of most voluminous batholithic magmatism in the Sierra Nevada. The Rb-Sr ages are generally consistent with the Sm-Nd ages, but are more scattered. The $^{87}Sr/^{86}Sr$ and $^{143}Nd/^{144}Nd$ intercepts of the igneous-textured xenoliths are similar to the ratios published for rocks outcroping in the central Sierra Nevada. We interpret the mafic/ultramafic xenoliths to be magmatically related to the upper- and mid-crustal granitoids as cumulates and/or restites. This more complete view of the vertical dimension in a batholith indicates that there is a large mass of mafic–ultramafic rocks at depth which complement the granitic batholiths, as predicted by mass balance calculations and experimental studies. The Sierran magmatism was a large scale process responsible for segregating a column of ~30 km thick granitoids from at least ~70 km of mainly olivine free mafic–ultramafic residues/cumulates. These rocks have resided under the batholith as granulite and eclogite facies rocks for at least 70 million years. The presence of this thick mafic–ultramafic keel also calls into question the existence of a "flat" (i.e., shallowly subducted) slab at Central California latitudes during Late Cretaceous–Early Cenozoic, in contrast to the southernmost Sierra Nevada and Mojave regions.

M. N. Ducea (✉) · J. B. Saleeby
California Institute of Technology,
Division of Geological and Planetary Science,
100-23, Pasadena, CA 911125, USA
Tel: 626-395-6590; Fax: 626-568-0935;
E-mail: ducea@gps.caltech.edu

Editorial responsibility: K. V. Hodges

Introduction

Our observations of magmatism in continental arcs and granitic batholiths come principally from upper- to mid-crustal levels exposed at the Earth's surface (e.g., Pitcher 1993). These observations are complemented by experimental studies of the plausible sources and liquid line of descent of arc magmas (Wyllie 1984). A similar kind of scientific information has provided a successful framework for understanding magmatism at mid ocean ridges (e.g., Klein and Langmuir 1987). However, a number of first order questions regarding the origin of large granitic batholiths cannot be answered by these constraints, in particular the balance of contributions from the mantle wedge underlying the arc, continental crust, and/or the subducting slab. This uncertainty leaves unresolved the extent to which the continental crust is internally differentiated through arc magmatism or generated by extraction from the sub-arc mantle.

What escapes our observation and prevents us from unique interpretations are the access to the roots of batholiths, the deep crustal counterparts of the plutons that we can observe to levels occasionally as deep as 30 km (Saleeby 1990), but in many regions only to ~5 to 10 km exposure depth. The crustal thickness beneath

modern magmatic continental arcs is more than 30 km. The Andes for example have a crustal thickness of 60 to 70 km in places (Isacks 1988). Some lower crustal rocks tectonically emplaced as terranes into the upper crust and exposed at the surface, may have attained their peak metamorphic conditions beneath continental arcs and may be petrologically related to the generation of arc magmas (Clemens 1988). However, since contemporaneous shallow level plutons or volcanic rocks are generally not preserved near these lower crustal exposures, the connection between lower and upper parts of continental arcs remains speculative. An exception could be the Kohistan arc of Pakistan (Coward et al. 1986) which exposes deep (40–50 km) as well as shallow levels of a Late Cretaceous–Eocene batholith.

Xenoliths brought to the surface by fast ascending mantle-derived magmas are another important source of information on the composition of the deep continental crust and underlying upper mantle (Rudnick 1992). Xenoliths can carry key petrogenetic information recorded in their mineralogy, textures, trace element concentrations and isotopic compositions, and also preserve a record of lower crustal history that can be unraveled using geochronological methods. Thus, xenolith studies can be an important means of studying the deep crust and upper mantle beneath arcs.

The Sierra Nevada mountain range, California, exposes a large Mesozoic composite Cordilleran batholith, one of the best studied batholiths on Earth (Bateman 1983). Several Miocene, extension-related mafic–intermediate volcanic centers (Moore and Dodge 1980), erupted though the axis of the Sierra Nevada batholith, contain xenoliths of lower crustal and upper mantle origin (e.g., Dodge and Bateman 1988). A number of mafic–ultramafic olivine-free xenoliths have equilibrated at depths of ~25 to 100 km (Mukhopadhyay 1989; Mukhopadhyay and Manton 1994; Dodge et al. 1986, 1988; Ducea and Saleeby 1996a). If proven to be cogenetic with the batholith, these samples represent a window into the lower crust and upper mantle of a rather typical Cordilleran batholith. Their trace element and isotopic compositions in particular could be important in distinguishing between various models of batholith generation. The first step to the success of such an approach is to demonstrate that these xenoliths are indeed cogenetic to the batholith. On the basis of their petrographic characteristics they could be also younger (Tertiary) cumulates in the lower crust, oceanic crustal fragments subducted under the Sierra Nevada, or possibly fragments of a lower crust totally unrelated to the surface batholith. In order to distinguish between these hypotheses, we determined the Sm-Nd and Rb-Sr ages, the $^{143}Nd/^{144}Nd$ and $^{87}Sr/^{86}Sr$ isochron intercepts, of nine samples from a suite of lower crustal and upper mantle xenoliths in the central Sierra Nevada. The results indicate a direct connection to the Sierra Nevada batholith outcrops for these xenoliths, and provide physical evidence of an ~100 km thick batholithic section.

The geology of the Sierra Nevada batholith – background information

Comprehensive information on the geology of the Sierra Nevada batholith can be found in recent reviews by Bateman (1983), Saleeby (1990) and references therein. We will briefly summarize the main petrologic and tectonic characteristics of the batholith. We will also provide an overview of the Tertiary xenolith-bearing volcanic rocks which erupted in the central part of the batholith.

The Sierra Nevada magmatic arc formed as a product of the prolonged ocean floor subduction beneath the southern edge of the north-American continent (Dickinson 1981). Magmatism took place in the Sierra Nevada between 220 Ma and 80 Ma (Everden and Kistler 1970; Chen and Moore 1982; Saleeby et al. 1987), although most of the exposed plutons yield ages between 125–85 Ma (Saleeby 1990). The batholith consists of numerous plutons ranging in size from less than 1 km^2 to over 100 km^2, with compositions that are mainly tonalitic to granodioritic and granitic; intermediate rocks (e.g., monzonites) or mafic rocks (e.g., gabbros) are found, but are not common even in the exposures of the deeper intrusion levels of the batholith. The batholith has a clear petrographic, chemical and isotopic west to east zonation, which is almost perpendicular to the batholith NNW–SSE long dimension (see Saleeby, 1990, for a review).

The batholith covers ~90% of the southern and central Sierra Nevada mountain range, and ~60–70% of the northern part of the range. Erosion, unroofing and tilting have taken place following magmatism. No significant metamorphic event has affected the Sierra Nevada batholith after its formation; igneous textures are preserved almost without exception. The igneous crystallization depths of the rocks presently exposed, vary from 0 km represented by large ~100 Ma caldera deposits preserved in the high Sierra Nevada (Saleeby 1990), to ~30 km in the southernmost Sierra Nevada (Pickett and Saleeby 1993). Igneous barometry studies have shown that the igneous crystallization depths gradually increase from north to south, as well as from east to west (Ague and Brimhall 1988; Ague 1997). Overall, the Sierra Nevada has been preserved as a tilted, but coherent block providing almost continuous exposures of the upper 30 km of a gigantic Mesozoic batholith.

There is no direct information on the composition and vertical extent of the batholith at depths exceeding the equivalent of 1.0 GPa equilibration pressures. Hence, the extent and composition of the batholith at depths greater than ~30–35 km can be inferred either indirectly from petrologic constraints borne out of studies of the granitoid outcrops or from geophysical observations.

The origin of magmas for the Sierra Nevada batholith is the subject of numerous debates. Before the gen-

eral acceptance of the plate tectonics theory, the batholith was thought to have formed by intracrustal melting at the deepest levels of an overthickened and strongly deformed "geosyncline" (Bateman and Eaton 1967). Models that incorporate melting of the mantle wedge above a subduction zone have been proposed for the batholith origin in more recent years (e.g., DePaolo 1981). The limitation of simple mantle melting models is that typical olivine-rich upper mantle compositions (peridotites) cannot produce granitoids by partial melting (e.g., Wyllie 1984). Either mafic melts generated in the mantle have later incorporated a large amount of preexisting continental crust (DePaolo 1981), large scale fractional crystallization led to the distillation of uppermost crustal granitoids while leaving behind large volumes of mafic cumulates (Coleman et al. 1992), or both. In either model presented above, a significant mass of low silica residua/cumulates, as much as ten times more than the "surface" batholith (>30 km thick), is predicted to exist at depth, depending on the composition of the source rocks in the crust and the proportion of "juvenile" material supplied from the mantle (Coleman and Glazner, 1998). The lower the silica concentration of the crustal source and the higher the mantle wedge contribution to the mass budget of the batholith, the larger the mass of the predicted residue will be. On the basis of experimental petrology (e.g., Green and Ringwood 1967; Wolf and Wyllie 1993; Rapp and Watson 1995), the material left behind as residues or cumulates will be rich in garnet, pyroxene, and possibly amphiboles, given the great depths at which most of it will be located.

However, there is no geophysical evidence for such a garnet-rich counterpart of the Sierra Nevada batholith at depth. A recent seismic profile across the Sierra Nevada demonstrated that the area has a thin, low velocity, granitic crust (35–42 km), which is underlain by upper mantle with properties of peridotite (Wernicke et al. 1996). Geophysical data do not support the existence of a garnet-rich layer beneath the seismologically defined crust.

The contradiction between the data emerging from petrologic and geophysical studies is an important one for understanding the origin of the batholith, and applies to other Cordilleran batholiths as well (e.g., the Peninsular Ranges batholith, Gromet and Silver 1987). Are some batholiths flat-bottomed and thin (Hamilton and Myers 1966) or have their roots been removed (Kay and Kay 1993)? A satisfactory answer may be obtained only when the vertical dimension of batholiths are compositionally "mapped" to depths much greater than allowed by surface exposures.

The Cenozoic collapse of the Cordillera at the latitude of the Sierra Nevada and the high magnitude extension to the east of the batholith in the Basin and Range province was accompanied by significant volcanism, which extended into the Sierra Nevada mountain range. As many as 150 small volume flows, pipes and dikes of mafic to intermediate compositions erupted through the central and southern Sierra Nevada batholith during the Late Cenozoic (Moore and Dodge 1980). The volcanism can be divided temporally in three stages: Miocene (8–12 million years), Pliocene (3–4 million years), and Quaternary (0–1 million years). Seventeen of these volcanic occurrences, representing all the three stages, contain upper mantle and/or lower crustal xenoliths (Ducea and Saleeby, 1996a, b). Five of the Miocene localities contain unusually rich populations of apparent lower crustal origin, including high pressure assemblages described as "garnet granulites" (some could be in reality garnet-bearing gabbroic cumulates), garnet websterites, eclogites, garnet clinopyroxenites and peridotites (Domenick et al. 1983; Dodge et al. 1986, 1988; Mukhopadhyay 1989; Ducea and Saleeby 1996a). In particular, the locality of Big Creek (Dodge et al. 1988), a trachyandesite pipe located in the central Sierra Nevada (lat: 37°13′N, long: 119°16′W), along the axis of the batholith, contains xenoliths that equilibrated at pressures as great as 4.2 GPa (Ducea and Saleeby 1996b). The feldspathic rocks (e.g., the "granulites") were interpreted to be cumulates of the Sierra Nevada batholith (Dodge et al. 1986), whereas the olivine-free and garnet-rich ("eclogitic") ultramafic assemblages, typically showing higher equilibration pressures, were interpreted as batholith cumulates (Mukhopadhyay 1989), or fragments of subducted oceanic crust (Dodge et al. 1988); but they could also be Tertiary cumulates related to the magmas that carried the xenoliths, or old lower crustal fragments that are unrelated to any of the above. The peridotites are thought to represent typical compositions of the deeper parts of the lithosphere beneath the Sierra Nevada (Ducea and Saleeby 1996a).

Petrography

Nine samples from a larger set previously investigated for thermobarometry (Ducea and Saleeby 1996a) were selected for geochronological analyses. They are four garnet clinopyroxenites and eclogites (with accessory orthopyroxene), one garnet websterite, two mafic feldspathic rocks, one metasedimentary rock and one garnet peridotite (Table 1). These compositional types cover the spectrum of lower crustal lithologies found as xenoliths at Big Creek, that resided at mid- to deep-crustal and upper mantle levels (30 km or more) beneath the batholith, and equilibrated over a large pressure interval, between 0.85 and 4.2 GPa. These samples were also selected because of their large grainsize, little if any alteration, and minor interaction between the host trachyandesite and the xenoliths. Figure 1 illustrates the textural appearance of the main petrographic groups investigated in this study: garnet clinopyroxenites and eclogites (Fig. 1a), garnet websterites (Fig. 1b), and feldspathic mafic rocks (Fig. 1c).

Four samples are composed mainly of garnet and clinopyroxenes (Table 1). In a more general sense, they are eclogite facies rocks with basic to ultrabasic chemistries. One sample (G36) has relatively high concentrations of Na_2O in clinopyroxene (2.5–3%) and a garnet with an almandine/pyrope ratio of 1.9 (group C garnet, according to Coleman et al. 1965), and resembles a "true eclogite", commonly found in, but not restricted to subduction environments. Sample BC207 contains a grossular-rich garnet and an augitic clinopyroxene, as well as accessory minerals such as sphene and calcite. The other two garnet-clinopyroxene rocks (BC218 and G39) contain group B garnets (Coleman et al. 1965) and Na-poor diopsidic pyroxenes. Garnet-clinopyroxene rocks

Table 1 Mineral composition, texture and petrography of the analyzed samples

Sample	Primary minerals[a]		Secondary minerals[b]	Alteration products	Reactions with host	Textures, structures	Rock type
	Principal (>1 vol. %)	Accessory (<1 vol. %)					
G36	GarB, cpx	Ru (in garB), hb, opx	Sp, kel	None	None	Cumulate[c], subhedral, poikilitc	Eclogite
BC218	Cpx, garB	Ru (in garB), hb, opx	Sp, kel	None	Hb-rich corona	Cumulate, subhedral, 120° triple junctions, poikilitic	Garnet clinopyroxenite
G39	Cpx, garB	Ru (in garB), opx, hb, qz, sp (?)	Sp (?), kel	None	None	Layering, poikilitic cpx in garB, anhedral	Garnet clinopyroxenite
BC207	GarC, cpx	Sph, ap, qz, mgt, opx	Kel, plg	None	None	Poikilitic cpx in garC, subhedral	Eclogite
F34	GarA, cpx, opx	Ap	Kel	None	Partial melting due to host heat	Layering, anhedral,	Garnet websterite
B75	Plg, garB, cpx	Ap, opx, qz, zr	Kel, sp, op	Turbid plg	Hb corona	Cumulate, layered, subhedral, 120^0 triple junctions, poikilitic	Layered gabbro
BC35	Plg, cpx, hb	Ap, op, qz	None	Cpx turbid coronas	Incipient melting of plg-hb contacts	Cumulate, layering, 120° equilibrium textures, subhedral	Layered gabbro
PBC	Ol, opx, cpx, gar		Kel, op	Cc	None	Porphyroclastic	Peridotite
297	Qz, cpx, garC	Sph, ru, zr, ap	Kel	None	Partial melting	Granoblastic	Quartzite

[a] *GarA*, *garB*, and *garC* garnet of type A, B, and C respectively from the classification scheme of Coleman et al. (1965), *cpx* clinopyroxene, *ru* rutile, *hb* hornblende, *ol* olivine, *sp* spinel, *kel* denotes a cryptocrystalline polymineralic breakdown product formed probably during the entrainment of the sample as xenoliths in the host melt, and consisting usually of plagioclase, spinel and an Al-rich orthopyroxene, *opx* orthopyroxene, *qz* quartz, *sph* sphene, *ap* apatite, *mgt* magnetite, *cc* calcite, *plg* plagioclase, *op* unidentified opaque minerals, *zr* zircon.

[b] These products appear to have formed after the inclusion of these samples in the host melt

[c] The term "cumulate" is used in this table. The term is strictly descriptive. These textures could be indicative of cumulate rocks formed during fractional crystallization in a magma chamber, but could also represent restites from a partial melting zone

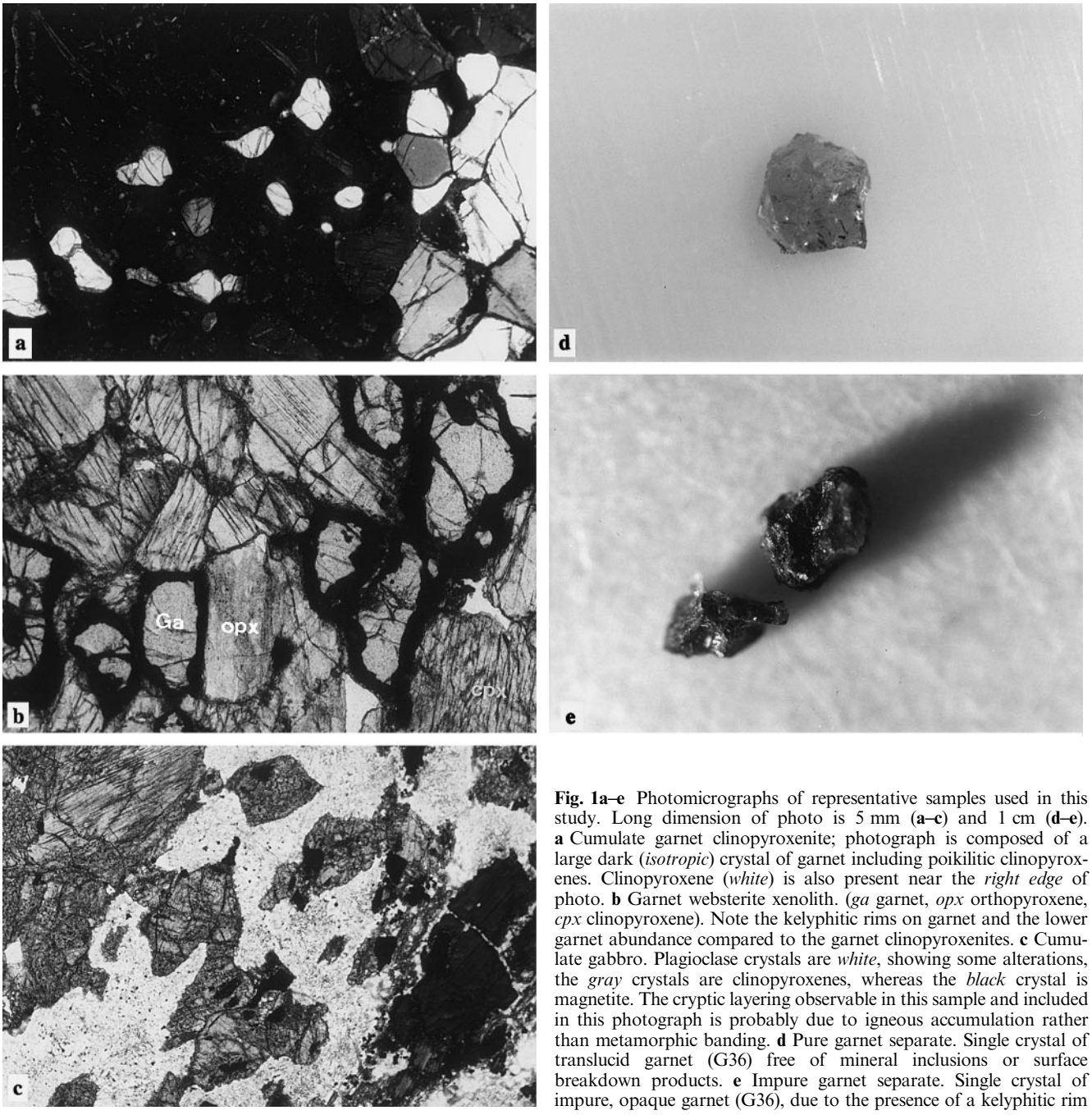

Fig. 1a–e Photomicrographs of representative samples used in this study. Long dimension of photo is 5 mm (**a–c**) and 1 cm (**d–e**). **a** Cumulate garnet clinopyroxenite; photograph is composed of a large dark (*isotropic*) crystal of garnet including poikilitic clinopyroxenes. Clinopyroxene (*white*) is also present near the *right edge* of photo. **b** Garnet websterite xenolith. (*ga* garnet, *opx* orthopyroxene, *cpx* clinopyroxene). Note the kelyphitic rims on garnet and the lower garnet abundance compared to the garnet clinopyroxenites. **c** Cumulate gabbro. Plagioclase crystals are *white*, showing some alterations, the *gray* crystals are clinopyroxenes, whereas the *black* crystal is magnetite. The cryptic layering observable in this sample and included in this photograph is probably due to igneous accumulation rather than metamorphic banding. **d** Pure garnet separate. Single crystal of translucid garnet (G36) free of mineral inclusions or surface breakdown products. **e** Impure garnet separate. Single crystal of impure, opaque garnet (G36), due to the presence of a kelyphitic rim

with such mineral compositions are commonly classified as "garnet clinopyroxenites", and are typically found in deep continental crustal environments (Carswell 1990). All four rocks contain accessory orthopyroxene and rutile (the last one mostly as inclusions in garnet). Other accessory minerals include hornblende, apatite, quartz. All samples have uniform mineral compositions (Ducea and Saleeby 1996a).

The textures of the 4 garnet clinopyroxenites and eclogites are very similar to the ones observed in igneous cumulates in stratified mafic magma chambers (Hunter 1986). The xenoliths studied here have attained textural equilibrium, and although the layering commonly faintly developed at xenolith scale (~5 cm scale) may be suggestive of metamorphic banding, the ubiquitous poikilitic inclusions leave little doubt that these rocks are igneous cumulates (Fig. 1a). The word "cumulate" is to be taken as a very broad term. These rocks may represent density-driven accumulations of crystals in a magma chamber, but they could also represent restites grown and compacted after the extraction of a large fraction of liquid (a "melanosome" in the migmatite terminology, Ashworth 1985). The textural relations alone are not enough to distinguish between these two scenarios.

Sample F34 is a garnet websterite (Fig. 1b). This rock yielded an equilibration pressure of 3.3 GPa, and is one of a number of high pressure garnet websterites (>2.5 GPa) found at Big Creek (Mukhopadhyay 1989; Ducea and Saleeby 1996a). There are a number of differences between garnet websterites and the garnet clinopyroxenites and eclogites: the abundance of orthopyroxene (20–30% in websterites compared to generally <1–3% in garnet clinopyroxenites and eclogites), the abundance of Cr in the clinopyroxene (>2% Cr_2O_3 in websterites, <1% Cr_2O_3 in eclogites),

the nature of the garnet (pyrope-rich or group A garnets of Coleman et al. 1965 in websterites, as opposed to group B garnets in eclogites), the pressure of equilibration (2.5–3.3 GPa in websterites, compared to <2.6 GPa in eclogites). The differences could reflect simply the different depth range from which these samples were equilibrated, but they could also be genetically unrelated. The textures of the websterites, including the sample analyzed for this study are however typical of cumulates, very similar to the garnet clinopyroxenites textures.

Samples BC75 and B35 are feldspar-rich rocks (Fig. 1c). Plagioclase constitutes about 50% by volume of the rock. Other minerals present are garnet and clinopyroxenes in BC75, and clinopyroxenes, hornblende and garnet in BC35. Rocks similar to BC75 and BC35 previously found at Big Creek (Dodge et al. 1986) and at the neighboring xenolith locality of Chinese Peak (Dodge et al. 1988) were described as "granulites". Trace element data indicate a cumulate/residual igneous origin for BC75 and BC35 (Ducea et al. 1997). Perhaps the best petrographic name for BC75 is "cumulate gabbro".

Sample 297 is a quartzite, whose protolith probably contained both calcareous and pelitic impurities, based on the high CaO and Al_2O_3 concentrations in the whole rock (Ducea et al. 1997). The rock contains ~90% quartz, ~8% diopside and grossular-rich garnet, and accessory sphene, rutile, zircon, and apatite. The rutile-sphene-grossular-kyanite barometer of Manning and Bohlen (1991) yields a minimum (no kyanite) equilibration pressure of 2.5 GPa assuming that rutile, sphene and grossular, which are usually not in contact but isolated within quartz-rich zones, were in equilibrium during their growth. The eclogite facies mineralogy of the aluminosilicate phases and the high concentrations of Al in sphene (M. N. Ducea and J. B. Saleeby, unpublished data) also suggest high depths of residence for this metasedimentary rock. This is the only sample from the suite analyzed in this study that does not display igneous, cumulate-like textures.

Sample PBC is a garnet peridotite which equilibrated at 4.2 GPa (Ducea and Saleeby 1996a). The rock contains by volume ~75% olivine, 15% orthopyroxene, 5% clinopyroxene and 5% garnet. The garnet is pyrope-rich, similar to garnets commonly found in kimberlites. The texture of this sample is porhyroclastic; grain size is ~1 mm in diameter, smaller than the other ultramafic (and mafic) xenoliths analyzed in this study. This xenolith also contains ~10% alteration products. It was included in this study because of the presence of clinopyroxene and garnet – which makes it suitable for Sm-Nd geochronology – and particularly because of the great depth at which it equilibrated.

A incipient metamorphic event, younger than the primary textures, resulted in partial breakdown of garnet and pyroxene from all the eight analyzed rocks. The products of this event are kelyphitic rims on garnet (a cryptocrystalline polymineralic product consisting of plagioclase, spinel, Al-rich orthopyroxene and anorthite) and the growth of a brown spinel at garnet-clinopyroxene contacts.

Analytical procedures

Whole-rock samples (typically 100–500 g) were carefully extracted from the host trachyandesite, broken down by hammer and crushed in a jaw crusher to about 1/3 of their average grainsize. Sample segments with visible alteration products were discarded. The samples were then homogenized and split, roughly two thirds for mineral separation, and a third for whole-rock analysis. Both splits were initially washed in deionized water and then acid leached for 25–30 min in warm 1 N distilled HCl, while in an ultrasonic bath. The whole-rock samples were then ground to a fine powder using a WC shatterbox prior to their dissolution. The split for mineral analyses remained relatively coarse throughout the separation procedure, although for some samples rich in composite grains, a few additional grinding steps were necessary. Separation of minerals was accomplished by a Franz magnetic separator and hand-picking in alcohol under a binocular microscope. The mineral separation procedure resulted in three fractions for each mineral: (1) ultrapure mineral separates; (2) lower purity separates, which contained occasional kelyphitic rims or very rarely, inclusions of other minerals; (3) impure fraction, with numerous composite grains. The third fraction was not used further for any analyses. We exemplify for garnet the difference between the first two fractions (Fig. 1d and e): the ultrapure fraction contained translucent grains with no stains or visible inclusions, whereas the lower purity fraction contained obvious black stains, the ubiquitous kelyphitic rims that accompany garnet. Although our aim was to analyze the purest grains for geochronology, we did analyze some separates of the lower "quality" to check whether their isotopic characteristics depart from the "pure" grains and if they carry any meaningful geochronometric information. The lower purity samples can be identified in Table 2 by the presence of the subscript "$_1$". To eliminate any grainboundary alteration effects, the hand-picked mineral separates were leached again in 2.5 N distilled HCl. The samples were then ultrasonically cleaned, rinsed multiple times with ultrapure water and dried in methanol.

The samples were spiked with ^{87}Rb, ^{84}Sr, and mixed ^{147}Sm-^{150}Nd tracers. Dissolution of the spiked samples for isotopic analyses was performed in screw-cap Teflon beakers using HF-HNO_3 (on hot plates) and HF-$HClO_3$ mixtures (in open beakers at room temperature). A few garnet separates were subjected to several, up to 5 dissolution steps before becoming residue-free. The samples were taken in 1 N HCl and any undissolved residue was attacked in the same way. Separation of the Rb, Sr, and the bulk of the REE was achieved via HCl elution in cation columns. Separation of Sm and Nd was carried out using a LNSpec® resin. The highest procedural blanks measured during the course of this study were: 11 pg Rb, 180 pg Sr, 5 pg Sm, and 18 pg Nd.

Isotopic analyses for Sr and Nd, as well as isotope dilution analyses of Rb, Sr, Sm, and Nd were performed at Caltech using a VG multiple collector mass spectrometer. The isotopic compositions of Sr and Nd were determined on the same spiked samples. The filament loading and mass spectrometric analysis procedures were similar to the ones previously described by Pickett and Saleeby (1994). The Sr isotopic ratios were normalized to $^{86}Sr/^{88}Sr = 0.1194$, whereas the Nd isotopic ratios were normalized to $^{146}Nd/^{144}Nd = 0.7219$. Estimated analytical $\pm 2\sigma$ uncertainties are: $^{87}Rb/^{86}Sr = 0.55\%$, $^{87}Sr/^{86}Sr = 0.0015\%$, $^{147}Sm/^{144}Nd = 0.8\%$, and $^{143}Nd/^{144}Nd = 0.002\%$. External reproducibility, based on the range of multiple runs of standard NBS987 (for Sr) and LaJolla Nd (for Nd) are estimated to be ± 0.000014 for Sr, and $\pm$ 0.00001 for Nd. Replicate analyses of two samples analyzed in this study (G36WR and BC207 WR) indicate similar reproducibility. The grand means of isotopic ratios were corrected by an off-line manipulation program, which adjusts for the spike contributions to both the fractionation correction and each ratio, and performs isotope dilution calculations.

Results

The Rb-Sr and Sm-Nd mineral and whole-rock analyses are given in Table 2. The geochronological results (Table 3 and Fig. 2) are principally constrained by the garnet and clinopyroxene isotopic compositions. The whole-rock values are potentially of interest because of the presence of accessory minerals such as apatite or sphene but are susceptible to exchange between xenolith and the host trachyandesite. In some cases, the results indicate the whole-rock splits were clearly infiltrated by the host magma. Some garnet mineral separates may contain minute inclusions of rutile which could not have been extracted during the sample preparation. However, even the garnet grains richest in rutile inclusions have less than ~1% (by volume) rutile. Since rutile is not a significant carrier of Rb, Sr, Sm and Nd, we believe that

Table 2 Isotopic data for mineral and whole-rock samples

Sample[a]	Rb (ppm)	Sr (ppm)	$^{87}Rb/^{86}Sr$	$^{87}Sr/^{86}Sr$	Sm (ppm)	Nd (ppm)	$^{147}Sm/^{144}Nd$	$^{143}Nd/^{144}Nd$	$\varepsilon_{nd}(0)$
Host-WR	78.51	348.2	0.334	0.705852	18.90	28.31	0.105	0.512532	−1.82
Eclogites									
G36-cpx	2.67	89.95	0.085	0.706290	1.79	3.62	0.299	0.512486	−2.96
G36-gar	1.83	3.24	1.626	0.708243	1.51	0.79	1.150	0.513008	7.21
G36-gar_1	2.47	10.45	0.679	0.706991	4.63	3.26	0.860	0.512850	6.04
G36-WR	8.66	113.68	0.219	0.706029	1.78	2.83	0.379	0.512547	−1.78
BC218-cpx	1.48	81.84	0.052	0.706239	0.77	0.78	0.594	0.512746	2.10
BC218-gar	3.05	5.87	1.493	0.707930	0.42	0.15	1.683	0.513352	8.92
BC218-WR	14.88	57.17	0.748	0.706452	0.92	0.92	0.605	0.512730	1.80
G39-cpx	2.01	76.94	0.075	0.706580	1.75	10.19	0.104	0.512387	−4.89
G39-gar	2.02	6.65	0.87	0.707085	12.51	29.00	0.261	0.512473	−3.21
G39-WR	1.98	70.32	0.081	0.706314	5.34	25.50	0.127	0.512392	−5.38
BC207-cpx	29.7	101.21	0.851	0.705895	0.17	0.80	0.129	0.512353	−6.54
BC207-hb	10.3	70.47	0.420	0.705353					
BC207-gar	5.8	8.37	1.981	0.706843	1.34	1.94	0.416	0.512558	−1.56
BC207-WR	15.1	53.55	0.810	0.705882	0.63	2.29	0.167	0.512403	−4.58
Websterite									
F34-cpx	0.19	208.07	0.003	0.705956	1.81	7.22	0.151	0.512468	−3.31
F34-cpx_1				0.705982				0.512581	
F34-opx	0.38	10.35	0.106	0.706383	0.17	0.54	0.194	0.512434	−3.99
F34-opx_1				0.706054				0.512579	
F34-gar	1.79	6.03	0.376	0.706616	1.07	0.92	0.700	0.512867	4.47
F34-gar_1				0.705940				0.512545	
F34-WR	1.93	158.30	0.035	0.705927	1.31	4.50	0.176	0.512462	−3.43
Mafic feldspathic rocks									
B75-cpx	0.66	80.33	0.023	0.705100	6.78	33.99	0.121	0.512669	0.60
B75-gar	0.27	0.93	0.838	0.707551	3.09	1.86	1.004	0.513125	9.49
B75-gar_1	2.68	30.36	0.254	0.706487	0.80	0.81	0.602	0.512866	4.46
B75-WR	6.10	190.44	0.091	0.705257	4.90	16.55	0.179	0.512689	0.61
BC35-cpx	0.197	48.10	0.012	0.707496	8.53	34.33	0.150	0.512321	−6.19
BC35-hb	1.03	27.86	0.037	0.708333	1.66	6.64	0.151	0.512346	−5.69
BC35-plg	10.23	1200.1	0.025	0.707348	12.50	9.89	0.764	0.512756	0.05
BC35-WR	5.73	659.01	0.025	0.707344	5.07	24.18	0.127	0.512344	−5.74
Garnet peridotite									
PBC-cpx					7.00	31.67	0.134	0.512491	−2.87
PBC-gar					0.88	0.63	0.848	0.512528	−2.14
PBC-WR	1.22	21.45	0.164	0.705580	0.28	0.65	0.261	0.512496	−2.70
Metasediment									
297-cpx	0.82	109.72	0.022	0.709232	1.45	8.37	0.105	0.511871	−14.96
297-gar	3.39	22.89	0.427	0.711981	2.20	1.72	0.776	0.512247	−18.02
297-WR	2.88	29.90	0.277	0.710763	2.01	10.40	0.117	0.512059	−11.29

[a] A petrographic description of the samples is given in the text. (*Host* Big Creek trachyandesite, *WR* whole rock, *cpx* clinopyroxene, *opx* orthopyroxene, *gar* garnet, *hb* hornblende, *plg* plagioclase). Mineral separates are super clean hand picked fractions except for the ones accompanied by the subscript "$_1$". The mineral samples with this subscript contained either small, but discernable inclusions of other minerals or kelyphitic rims

even if such inclusions went undetected in the "garnet" separates, they did not significantly affect the geochronology data.

When only two points were used for calculating an "age", the 2σ uncertainty (given in Table 3) is entirely analytical. However, only when 3 or more points are regressed, can one assess whether the best-fit line is a statistically valid isochron. For 3 or 4 point regression lines we calculated the mean squared weighted deviation (MSWD; York 1969). Wendt and Carl (1991) show that if the calculated MSWD is close enough to 1 (up to 3–4 for the data used in this study) the regression line is statistically justified to represent an isochron. The values of MSWD for the Nd data presented in this study are typically < 4, whereas the MSWD for Sr data are > 25 (Table 3). Therefore, the Nd data are likely to have geochronological significance, whereas the Sr data may not.

The garnet peridotite PBC yields a Miocene Nd age (10 ± 15 Ma) indicating that this sample was undergoing active recrystallization at the time of entrainment (8.3 Ma, Dodge et al. 1988). The Sr and Nd ages for all other samples but the quartzite 297 are Mesozoic–Early Cenozoic, between 44.5 Ma and 214 Ma (Fig. 2).

Table 3 Grainsize, thermobarometric conditions, and Rb-Sr and Sm-Nd ages determined for the analyzed samples

Sample	Grainsize (mm)[a]	Pressure[b] (GPa)	Temperature[c] (°C)	Rb-Sr age[d]	$^{87}Sr/^{86}Sr$ intercept	MSWD[e]	Sm-Nd age	$^{143}Nd/^{144}Nd$ intercept	MSWD[5]
G36	2.5	1.5 (Mk)	770 (EG)	89.4 ± 0.90 (gar-cpx)	0.70618		93.7 ± 0.8 (gar-cpx)	0.51230	
		1.4 (HG)		91.0 ± 55 (gar-cpx-WR)	0.70596	2020	92.8 ± 3.5 (gar-cpx-WR)	0.51231	1.32
BC218	4.5	1.6 (Mk)	725 (EG)	82.4 ± 0.96 (gar-cpx)	0.70618		85.1 ± 1.3 (gar-cpx)	0.51242	
				83.0 ± 433 (gar-cpx-WR)	0.70597	4840	86.6 ± 14.5 (gar-cpx-WR))	0.51240	3.67
G39	5.0	2.2 (HG)	675 (EG)	44.72 ± 1.74 (gar-cpx)	0.70623		83.7 ± 1.4 (gar-cpx)	0.51233	
		2.0 (Mk)		55.6 ± 165 (gar-cpx-WR)	0.70638	735	86.7 ± 11 (gar-cpx-WR)	0.51232	0.55
BC207	2.5	1.9 (HG)	650 (PN)	67.2 ± 1.0 (gar-cpx)	0.70518		109.2 ± 5.0 (gar-cpx)	0.51219	
		1.7 (Mk)		64.5 ± 25 (gar-cpx-hb-WR)	0.70506	189	121.2 ± 30 (gar-cpx-WR)	0.51223	5.52
F34	3.5	3.3 (HG)	860 (H)	124.6 ± 3.69 (gar-cpx)	0.70595		111.1 ± 5.2 (gar-cpx)	0.51236	
				126 ± 80 (gar-cpx-opx-WR)	0.70599	610	120 ± 30 (gar-cpx-opx-WR)	0.51232	7.20
B75	2.5	0.98 (NP)	920 (EG)	213.3 ± 1.70 (gar-cpx)	0.70503		79.0 ± 1.20 (gar-cpx)	0.51261	
				214 ± 49 (gar-cpx-WR)	0.70501	24.6	80.0 ± 3.12 (gar-cpx-WR)	0.51259	1.28
BC35	3.0	0.84 (NP)	872 (EG)	–	–	–	102.8 ± 23.0 (cpx-hb-plg-WR)	0.51224	3.42
PBC	0.7	4.2 (HG)	975 (EG)	–	0.70492	–	10 ± 15 (gar-cpx)	0.51249	
297	0.3	2.5 (Mn)	645 (PN)	477.4 ± 3.4 (gar-cpx)	0.70908		85.7 ± 3.2 (gar-cpx)	0.51181	

[a] Rock average
[b] The following thermodynamic calibrations were used for pressure determinations (see also Ducea and Saleeby, 1996a): *Mk* Mukhopadhyay (1991), *HG* Harley and Green (1982), *NP* Newton and Perkins (1982), *M* Manning and Bohlen (1991)
[c] The following calibrations were used for temperature determinations (see also Ducea and Saleeby, 1996a): *EG* Ellis and Green (1979), *H* Harley (1984), *PN* Pattison and Newton (1989)
[d] The isochrons are based exclusively on the mineral data of highest purity listed in Table 2. The uncertainties are 2σ values. Abbreviations are as in Table 2
[e] Mean squared weighted deviation (York 1969; Wendt and Carl 1991), calculated for 3 or more points using the program provided by Ludwig (1991)

Fig. 2A-B Mineral isochrons for the (**A**) Sm-Nd and (**B**) Rb-Sr systems. Sample PBC which yields an entrainment age (Miocene) is not plotted. The isochrons have been fitted through data points with or without taking into account the whole-rock values, as explained in text. The ages marked near the isochrons are in Ma. The size of the symbols is approximately three times as large as the analytical uncertainties. We used the following decay constants: $\lambda_{Rb} = 1.42 \times 10^{-11}\ a^{-1}$, and $\lambda_{Sm} = 6.54 \times 10^{-12}\ a^{-1}$

Quartzite 297 has a Sr slope corresponding to an "age" of 471 Ma. No Sr mineral isochron could be calculated for sample BC35 using the available data in the absence of garnet from our dataset. The Nd mineral ages, including quartzite 297 fall within a much tighter interval, between 80 Ma and 120 Ma. These values and similarity of the Nd ages are indicative of a relationship between the surface batholith and these lower crustal rocks. Three Sr ages (samples G36, BC218, and F34) are sim-

ilar to the Nd ages calculated on the same samples, reinforcing the previous statement. The spread of the other four Sr ages suggests a more complicated history and to a first degree at least, these ages have to be considered suspicious. We noticed the high concentrations of Rb and Sr in some mineral separates compared to previously analyzed xenolith garnets and pyroxenes (e.g. Wendtland et al. 1996). We fear that part of the problem with the Rb-Sr system is the failure to obtain absolutely clean mineral separates with respect to Rb and Sr. For example, the concentrations of Rb in garnets and pyroxenes are expected to be low (~1 ppm) in eclogites and granulites, whereas some of our samples have higher Rb concentrations. The most outstanding is sample BC207, with ~30 ppm Rb in clinopyroxene, and 5.8 ppm Rb measured in garnet.

The Sr and Nd intercepts (Table 3) are very similar for all samples except for quartzite 297. The $^{87}Sr/^{86}Sr$ "initials" of the seven olivine-free mafic/ultramafic rocks vary between 0.70501 and 0.70623, very much like the initial Sr ratios in the surface batholith rocks in the central Sierra Nevada (average central Sierra Nevada batholith $^{87}Sr/^{86}Sr_{100} = 0.7057$, Kistler and Peterman 1973, 1978). The $^{143}Nd/^{144}Nd$ ratios of the seven olivine-free mafic/ultramafic rocks fall between 0.51232 and 0.51239, also very similar to the $^{143}Nd/^{144}Nd_{100}$ surface batholith average of 0.51234 in the central Sierra Nevada (DePaolo, 1981). The quartzite has somewhat higher $^{87}Sr/^{86}Sr$ and lower $^{143}Nd/^{144}Nd$ ratios, 0.7095 and 0.51182 respectively (at 100 Ma). Peridotite PBC has $^{87}Sr/^{86}Sr$ and $^{143}Nd/^{144}Nd$ ratios characteristic of the enriched mantle lithosphere known to exist beneath the Sierra Nevada (e.g., Mukhopadhyay and Manton 1994).

Data interpretation

The two geochronometric systems used in this study have: (1) an extremely favorable spread of Rb/Sr and particularly Sm/Nd ratios between pyroxene and garnet; (2) high closure temperatures in garnet-bearing lower crustal rocks (e.g., Jagoutz, 1998; Coghlan 1990; Metzger et al. 1992). Aware of the limitations of establishing lower crustal ages on xenoliths and the rather limited number of minerals available in the Sierran xenoliths, we have attempted to obtain useful geochronological information without necessarily expecting the high precisions and accuracies typical for the Rb-Sr or Sm-Nd results when applied to surface rocks. In our case, we searched for the bulk age of the lower crust: is it Paleozoic, Precambrian, is it batholith related, are the ages scattered throughout the Mesozoic or clustered toward the end period of Mesozoic magmatism, or perhaps are they approaching the age of the Miocene volcanic host rock? Are these samples broadly cogentic, or do they exhibit a large spectrum of ages and initial ratios?

Deep crustal and upper mantle rocks sampled as xenoliths are commonly residing at temperatures above the closure temperatures (Dodson 1973) for most geochronometers (Rudnick 1992). The "ages" locked-in by such xenoliths will accordingly reflect the age of entrainment, i.e., the age of the host volcanic carrier. Xenoliths analyzed in this study equilibrated between ~650–950 °C (Table 3); these numbers suggest that at the time of entrainment, the xenoliths were equilibrated at temperatures ≤650–950 °C. The closure temperature of REE and Sr in garnets and pyroxenes can be calculated as a function of cooling rates (Dodson 1973), using available experimental data from Sneeringer et al. (1984) and Coghlan (1990). The results of this calculation for spherical grains having diameters of 0.6 cm are shown in Fig. 3 as a function of cooling rate, and are compared to the range of equilibration temperatures measured in the samples analyzed in this study. It is likely that the abundant mineral with the more sluggish kinetics, clinopyroxene in this case, will control the closure temperature (Metzger et al. 1992). The equilibration temperatures measured on xenoliths and the predicted closure temperatures for REE and Sr indicate that in the case of Sierra Nevada xenoliths studied here, there is a distinct possibility that most of the samples were not above the closure temperature at the time of entrainment. Hence, the Sierran xenoliths may carry Nd and Sr geochronometric information able to date the most recent lithospheric thermal event that was imprinted on them, instead of simply recording the age of xenolith entrainment. All xenoliths excepting the garnet peridotite PBC display significant Rb-Sr and Sm-Nd isotopic mineral disequilibria which confirm this prediction.

We interpret the Sm-Nd ages reported in Table 3 to record the time when these xenoliths cooled below the closure temperatures of this particular system. Most regression lines involving 3 or more points are charac-

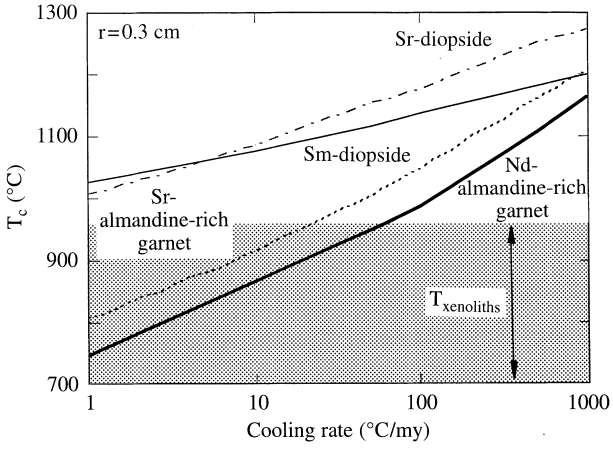

Fig. 3 Predicted closure temperatures (°C) of diopside and almandine-rich garnet as a function of cooling rate (°C/million years) for the Sr and Nd systems. Relevant diffusional parameters are from Sneeringer et al. (1984) for Sr and Sm (as a proxy for Nd) in diopside and from Coghlan (1990) for Sr and Nd in garnets. The closure temperatures are calculated as in Dodson (1973), assuming spherical grains with a radius of 3 cm. The range of equilibration temperatures measured in the xenoliths in this study ($T_{xenoliths}$) is shown as a *shaded field*

terized by MSWD values (Table 3) close enough to 1 to be considered "isochrons" (Wendt and Carl 1991). In some cases the whole-rock ratios have been modified by interaction with the host trachyandesite (Fig. 4a, b). More specifically, we suspect that physically the split "xenolith whole rock" has been polluted by some small, undetected amounts of the host trachyandesite. The whole rocks have been crushed to powders, and despite the cautions that we have taken in sample preparation (see "Analytical procedures"), they could contain some intergranular material inherited from the host trachyandesite. However, the whole-rock isotopic ratios of $^{143}Nd/^{144}Nd$ and $^{147}Sm/^{144}Nd$ are very similar to those of the clinopyroxenes, because clinopyroxene is the abundant mineral richest in Sm and Nd. From this perspective, the departure of some of the whole-rock ratios toward the host trachyandesite is not very relevant; the clean, pure clinopyroxene fractions are better samples of the low Sm/Nd end of the isochrons.

In contrast to the Sm-Nd system, none of the Rb-Sr regression lines based on three points or more are "isochrons". The MSWD values of all Sr errorchrons are >25. The three-point ages calculated using the Rb-Sr chronometer may or may not have geologic significance. We separate the two-point (garnet-clinopyroxene) Rb-Sr "ages" into three groups, by comparison to the Nd ages. Three samples, G36, BC218, and F34 yield indistinguishable Sr and Nd ages (group I), two samples, G39 and BC207 yield younger Sr ages (44, and 65, respectively) than Nd ages (group II), while BC75 and 297 yield anomalously high Rb-Sr ages, 211, and 477, respectively (group III). Below we will speculate on the possible geologic significance of the Sr data.

We interpret the group I Sr ages as igneous or slightly post-igneous values for these cumulates, based on the coincidence with the Cretaceous magmatic peak of the Sierra Nevada batholith and the similarity with their corresponding Nd ages. Based on textural arguments and the lack of any product suggesting the presence of fluid phases in these rocks, it appears likely that the isotopic equilibration between garnet and pyroxenes in these rocks was entirely diffusional. The similarity between the Sr and Nd ages in these samples is what ex-

Fig. 4 a Nd isochron of sample 297, illustrating the contamination of the xenolith whole-rock powder by the host trachyandesite; the whole-rock $^{147}Sm/^{144}Nd$ and $^{143}Nd/^{144}Nd$ ratios of the analyzed "whole rock" are located along a mixing line (*dashed line* in the figure) between the host rock and the true location of the whole rock along the Nd isochron (*solid line*). **b** Sr isochron of sample G36 illustrating, similarly to **a,** the contamination of the xenolith "whole-rock" powder by the trachyandesite. **c** Nd isochron of BC75 including the kelyphitic garnet (gar_1) separate; gar_1 lies close to the mineral isochron. **d** Sr isochron of BC75, including kelyphitic garnet (gar_1); in contrast to **c,** the kelyphite lies off the mineral isochron indicating open system breakdown of garnet in the presence of the Sr-rich, Nd-poor phase, possibly an aqueous phase

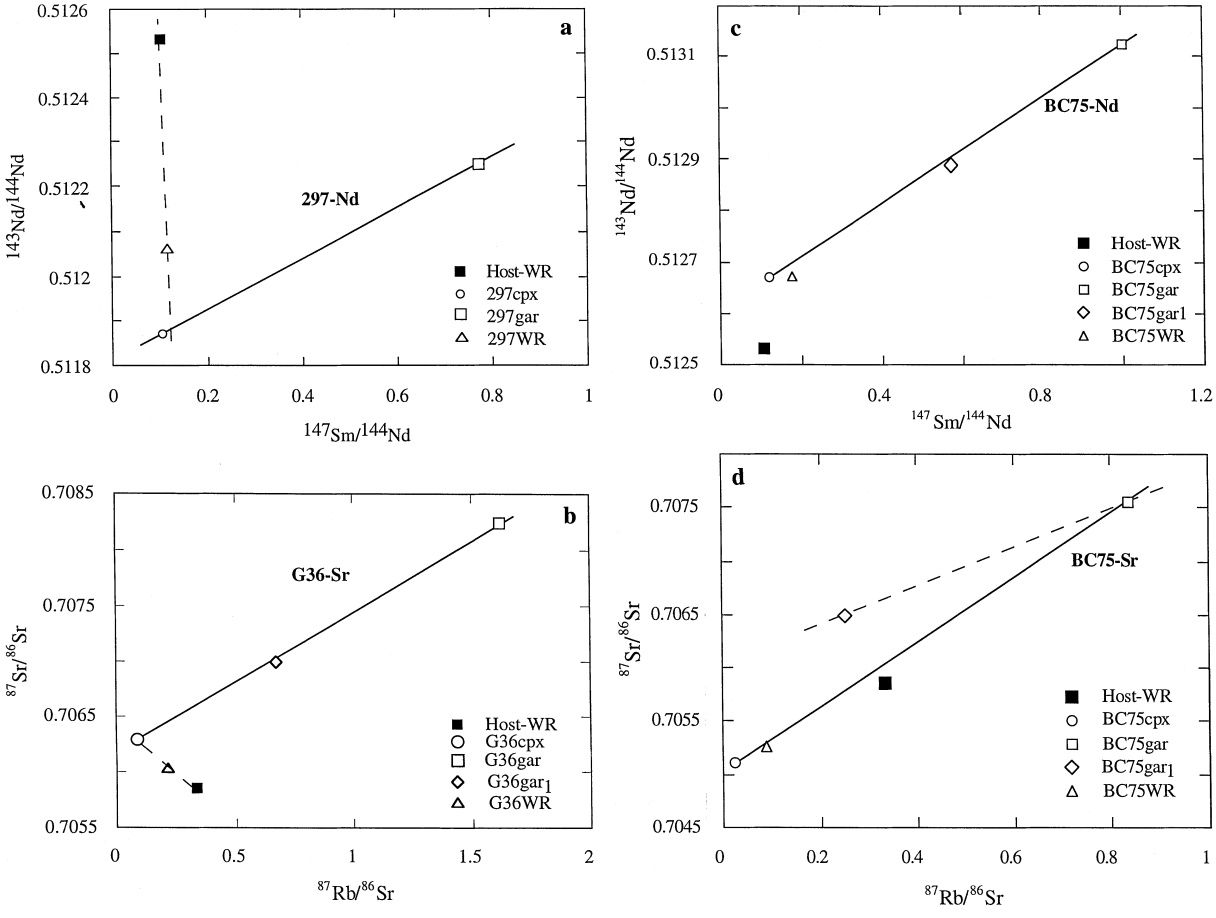

perimental data on Sr and Nd diffusion in garnet predicts for the geologic scenario envisioned above (Harrison and Wood 1980; Coghlan 1990; Burton et al. 1995). The failure of the Sr system to define statistically valid isochrons indicates however that this geochronometer is not particularly reliable when applied to these deep lithospheric xenoliths.

Group II and III dates may not have any geologic significance. Below we outline a number of scenarios which may have led to group II "ages". These "ages" are consistent with the batholith derivation of these samples, but require some resetting of the Rb-Sr system at 44–65 Ma, partial resetting at a time younger than 44–65 Ma, or disturbance in a geochronologically meaningless fashion, such as exchange with a fluid phase. We have not observed petrographic evidence for alteration or metamorphic reactions in the presence of a fluid phase. However, the most vulnerable points on the Sr isochrons presented here are the garnets. The slope of a garnet-clinopyroxene Sr isochron can be perturbed by interaction with small fractions of a component that plots away from the isochron. The Sr "ages" will artificially either be decreased or increased, depending on whether the fluid plots below or above the isochron at the time of perturbation. The group III Sr dates are even more difficult to interpret. It is possible that interaction with the host trachyandesite has modified the original Rb/Sr and $^{87}Sr/^{86}Sr$ ratios of the clinopyroxene and the whole-rock in sample 297. Such a process could also explain the low quality of the Nd whole-rock isotope ratios for the same sample. However, it does not appear that the same explanation can hold for B75 (Fig. 2) because the host rock isotopic ratios are nearly collinear to the B75 Sr isochron.

Overall, our Sm-Nd results indicate that the samples equilibrated during the most prolific igneous period in the Sierra Nevada batholith (Chen and Moore 1982). Furthermore, our data confirm the previous geochronological results on lower crustal xenoliths (Wendtland et al. 1996), indicating that the Sm-Nd system is quite a robust xenolith chronometer, while the Rb-Sr system is not.

We have also analyzed the isotopic compositions of the kelyphitic rim-bearing garnets for a few samples (Table 2) in order to test if kelyphitization is a closed system effect (simple garnet breakdown, or breakdown reaction involving surrounding clinopyroxenes) or if it requires the presence of an additional component, foreign to the eclogite or gabbro. Neodymium isotopes on kelyphitic garnets for samples BC75 (shown in Fig. 4c) and G36 indicate a closed system behavior. A similar result is indicated by the Sr isotopes in the kelyphitic garnets of sample G36. The Sr isotopes of the "$garnet_1$" fraction of sample BC75 depart from the reported Sr isochron for that sample (Fig. 4d), suggesting an open system behavior of Sr during kelyphite formation in this sample. More analyses are required in order to assess whether kelyphitization is an open system process with respect to the xenolith samples and whether the kelyphites carry any geochronologic information.

Petrologic and tectonic implications

The petrographic, thermobarometric and geochronologic results presented above refine our information on the composition of the central Sierra Nevada batholith at depth. We will relate the geology of the surface batholith with the lower crustal and upper mantle rocks and put constraints on the gross crustal structure of the batholith. The central Sierra Nevada Mesozoic crustal section, especially the lower half appears to be radically different from the one observed in the southernmost Sierra; we will define the differences between the two sections and address their regional tectonic implications.

Batholith residua/cumulate origin for the xenoliths

As mentioned above, the Sierra Nevada provides surface exposures of a composite Mesozoic batholith over a thickness of 30 km. Mafic and ultramafic xenoliths which equilibrated at depths of 35–100 km beneath the central batholithic exposures yield Sm-Nd ages which fall within the age range of 90% of the Sierra Nevada plutons (Fig. 5). The mineral isochron intercepts for Sr and Nd (Table 3) as well as age-corrected whole-rock Sr and Nd isotopic ratios obtained on similar xenoliths (Dodge et al. 1986, 1988; Mukhopadhyay 1989; Ducea and Saleeby 1996b) have values similar to the initial Sr and Nd isotopic ratios (Kistler and Peterman 1978; DePaolo 1981) of the surface batholith in the central Sierra Nevada (Fig. 6). In addition, $\delta^{18}O$ ratios measured on the same xenoliths analyzed in this study (Ducea et al. 1997) are practically identical to the range of values measured in the central Sierra granitoids (Masi et al. 1981). These results establish a broad cogenetic relation between the surface batholith and its lower crust/uppermost mantle. The major and trace element compositions of the seven igneous-textured samples presented in this study are inconsistent with them being frozen melts (Ducea et al. 1998); instead these rocks are residual assemblages (either restite or cumulates) left behind after the extraction of granitoids.

The strongly fractionated REE patterns ($La_n/Yb_n \geq 10$–15) and minuscule Eu anomalies in most of the central Sierra Nevada plutons (Dodge et al. 1982) indicate that garnet is an important phase in the granitoid melt residue, while the role of plagioclase as residual phase is minor. These data suggest that central Sierra Nevada granitoids were formed by melting a relatively deep reservoir, located at 35–40 km or more (Green and Ringwood 1967). The presence of a garnet-pyroxene-(amphibole) keel beneath the central Sierra Nevada batholith, as suggested by the xenolith compositions, is consistent with these constraints. Several experimental studies have documented that garnet-pyroxenes (±amphibole) assemblages represent the residual assemblages after extracting granitoid melts from a wet basaltic protolith at pressures exceeding

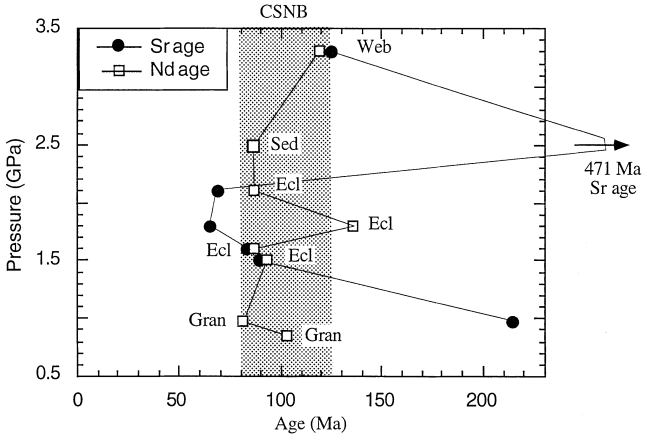

Fig. 5 Sample Sr and Nd ages versus equilibration pressures. Note there are three samples that yield almost identical Sr and Nd ages, while others do not. No correlation between ages and crustal depth is evident in our dataset. *Shaded field labeled "CSNB"* represents the time interval comprising ~90% of the ages yielded by surface plutons in the central Sierra Nevada batholith (summarized by Saleeby, 1990) (*ecl* eclogites and garnet clinopyroxenites, *gran* granulites and cumulate gabbros, *sed* metasedimentary rock, *web* websterite

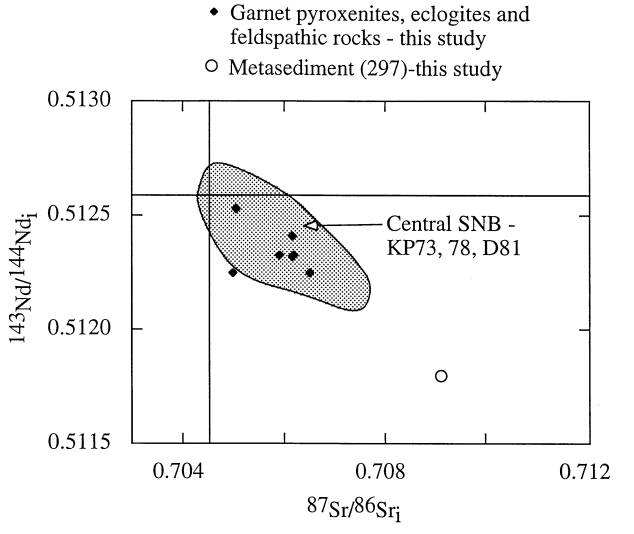

Fig. 6 Initial $^{143}Nd/^{144}Nd$ versus $^{87}Sr/^{86}Sr$ for the analyzed samples, compared to the field of central SNB (Kistler and Peterman 1973, 1978, abbreviated in the figure as *KP73*, *78*; and DePaolo, 1981, abbreviated as *D81*).

1 GPa (e.g., Wolf and Wyllie 1993; Rapp and Watson 1995). Moreover, the mineral compositions of the experimental residues are within the range of mineral compositions encountered in the ultramafic rocks analyzed in this study (Ducea and Saleeby 1996a).

The origin of the batholith source rocks can be constrained by the isotopic ratios in the residual assemblages and granitoids. The low, negative initial values of ε_{Nd} (< 1.8) argue against derivation of all these eclogite facies rocks from oceanic crust or a young, depleted mantle. A significant component involved in the mass budget of the Sierra Nevada batholith must be represented by Precambrian lower crustal and/or lithospheric (isotopically enriched) mantle, as suggested by the low, mostly negative initial values of ε_{Nd} (~−5.5 to 1.8) and the relatively low $^{87}Sr/^{86}Sr$ (~0.705–0.706) ratios. Other lines of evidence support this assertion, e.g., the common presence of Precambrian inheritance in zircons from the central Sierra granitoids (Chen and Tilton 1991). Texturally and thermochronologically however, the mafic–ultramafic xenoliths have a "memory" limited by the extensive melting process in which they were involved during the Cretaceous. Consequently, the ages measured on the feldspathic and eclogitic xenoliths are most likely near-igneous cooling ages. Sample 297 may be a good example of a preexisting crustal rock which did not experience melting during the batholith formation. Even so, the Nd age of this sample was reset during the Late Cretaceous thermal pulse, whereas its Sr may have only partially been reset.

A proposed vertical section through the Sierra Nevada lithosphere

The composition of the Sierra Nevada batholith can be constrained reasonably well from surface exposures and geophysical data down to ~30 km (Saleeby, 1990). Assuming that the xenolith lithologies are representative for the depths at which they equilibrated, we will extend downward the idealized vertical compositional column through the Sierra Nevada lithosphere.

The xenolith results show that a thick (70 km, possibly more) sequence of residual/cumulate mafic to ultramafic rocks complement the upper- to mid-crustal rocks of the batholith (Fig. 7). Below we will outline some characteristics of the upper crust, the upper crustal to lower crustal transition, the lower crust, the crust-mantle boundary, and the upper mantle from beneath the Mesozoic Sierra Nevada batholith.

The upper 30 km of the Sierra Nevada crust consist almost entirely of tonalites, granodiorites, and granites. This statement appears to hold even for the batholith exposures from the Tehachapi Mountains in the southernmost Sierra, at igneous exposure depths of 20–30 km (Pickett and Saleeby 1993). Saleeby (1990) reports an average silica concentration of 60% for the Tehachapi exposures, slightly less siliceous than the bulk Sierra Nevada exposures, ~65% SiO_2 (Bateman and Dodge 1970). A recent seismic refraction experiment across the Sierra Nevada (Wernicke et al. 1996) shows that the seismic velocities remain fairly low (v_p = 6–6.4 km/s) throughout the seismologically defined crust, ~35 km thick (Fliedner and Ruppert 1996). Such low seismic velocities are characteristic for silica-rich, "granitic" rocks. The geophysical data is therefore consistent with geological evidence indicating that the upper 30–35 km of the Sierran lithosphere consists mainly of granitoids.

The transition between the granitic upper crust and deeper, more mafic lithologies occurs between 30–40 km. If the xenolith data are representative for the

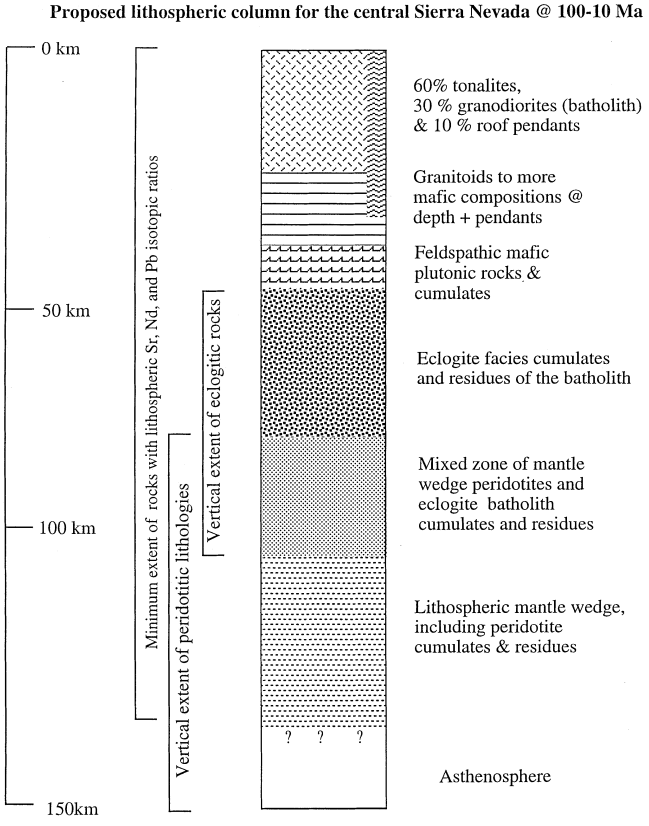

Fig. 7 Schematic lithospheric column for the region underlying the central SNB, based on outcrop and xenolith studies (see text)

crustal section they sampled, it appears that mafic rocks become progressively abundant in the 0.8 to 1.2 GPa interval. Feldspathic xenoliths with intermediate to mafic compositions generally display equilibration pressures lower than 1.2 GPa, whereas feldspar-free, mainly mafic rocks such as garnet clinopyroxenites and websterites equilibrated at pressures always higher than 1.0 GPa. A few xenoliths whose pressure of equilibration was calculated to be in the ~1.0–1.4 GPa interval are cumulates with alternating feldspar-rich and garnet-pyroxene-rich layers (e.g., sample B75 from this study).

Rocks that equilibrated at pressures higher than 1.5 GPa consist mainly of garnet, one or two pyroxenes, and amphibole. Garnet clinopyroxenites represent the most common deep xenolith rock type sampled at Big Creek and similar Miocene xenolith localities from the central Sierra Nevada. Rocks of broadly similar compositions are commonly found included as veins, pods or irregular bodies in larger volumes of garnet and spinel peridotites, for example in Alpine peridotites' (Carswell 1990). By analogy with the Alpine peridotites' field relationships, one could interpret the pyroxenites as mantle-derived, relatively small volume inclusions in peridotites. The composite feldspathic-garnet pyroxenitic cumulate xenoliths described above, as well as the scarcity of spinel peridotitic xenoliths (which equilibrated at pressures lower than ~2.5 GPa, Ducea and Saleeby 1996a), all argue for the existence of an "eclogitic"-rich layer somewhere between ~40–75 km beneath the Sierra Nevada. This layer corresponds in our view with the level at which large magma chambers have mixed mantle and crustal magmatic components during the Mesozoic, have distilled the Sierra Nevada granitoids, and stored large volumes of garnet-rich cumulates/restites.

A lower crustal to upper mantle transition is hard to define beneath the Sierra Nevada, and perhaps beneath any batholith (Pitcher 1993). Our deepest samples from Big Creek equilibrated at pressures between 2.5 and 4.2 GPa (Ducea and Saleeby 1996b), and comprise mainly garnet-bearing peridotites and garnet websterites, suggesting that both pyroxenites (broadly "eclogites") and peridotites are present at depths of ~75–100 km. Presumably at greater depth peridotitic rocks predominate over pyroxenites. It is interesting to note that our garnet websterite sample F34, which equilibrated at ~100 km yielded synbatholithic Sm-Nd and Rb-Sr ages and batholith-like Sr and Nd intercepts. A Mesozoic age measured on F34 is consistent with the progressive development of a cold and thick lithosphere beneath the Sierra Nevada during the vanishing stages and after the cessation of magmatism. It is also worth noting that the deepest sample recovered from Big Creek, garnet peridotite PBC has isotopic characteristics of lithosphere and locked-in a relatively low temperature of 975 °C (Ducea and Saleeby 1996a, b). This sample yields Miocene Nd and Sr ages probably because of its long term residence near or above the closure temperature for these two systems, and possibly also because of its relatively fine grain size. These results suggest that the Mesozoic to Miocene lithosphere was at least 130 km thick beneath the central Sierra Nevada. The development of a cold and rather thick lithosphere during the late stages and following the cessation of magmatism in a large continental batholith is somewhat surprising, but these results are consistent with the anomalously low Sierra Nevada heat flow throughout the Cenozoic (Dumitru 1990) postulated from fission track studies, and measured in the western half of the range (Lachenbruch 1968).

Two implications emerging from our interpreted lithospheric column may have important tectonic implications and will be outlined below: (1) the vertical scale at which batholith-related magmatism operates; (2) the efficiency of segregating light granitic crust from dense residues during batholithic magmatism.

1. Our data demonstrate that igneous products cogenetic with the Late Cretaceous Sierra Nevada batholith can be found from surface levels to at least ~100 km depth. These results indicate that batholithic magmatism (at least in the Sierra Nevada) is a lithospheric scale process capable of isotopically homogenizing and thermochronologically resetting at least a 100 km thick lithosphere in a relatively short period of time (a few tens of millions of years). The crustal column is characterized by a coherent large scale major element chemical heterogeneity, typical for suites of consanguineous igneous rocks.

2. It is remarkable how well the two entities, upper- to mid-crustal tonalites and granodiorites and the deep crustal/mantle mafic–ultramafic rocks appear to be spatially separated. Very often petrologists ask how much mass has been extracted out of the mantle during batholith formation, a question of relevance to the origin of continents. Data presented here provide us with a potentially useful constraint in understanding crustal growth: regardless of how much mass is recycled versus juvenile, the Sierra Nevada batholith has efficiently "distilled" granitoids from a thick, mainly "eclogitic" residual mafic–ultramafic mass.

No flat slab beneath the central Sierra Nevada

The data presented above show that a 100 or more km thick section which can be related to the Sierra Nevada batholith, has resided at least between the Mesozoic and Mid-Miocene times under the Sierra Nevada. The low ε_{Nd} values of the feldspathic and "eclogitic" rocks (ε_{Nd} initial < 1.8) argue strongly against an oceanic crustal origin. Olivine-rich, garnet-bearing ultramafic rocks probably become progressively abundant at deeper levels. Garnet peridotite inclusions from the pipes of Big Creek and the neighboring Pick and Shovel and Camp Sierra locations, all display continental lithospheric mantle isotopic signatures (Mukhopadhyay and Manton 1994; this study). We have no xenolith evidence for the existence of any rocks of oceanic plate derivation at any time between the Mesozoic and Mid-Miocene at least for ~130 km below the central Sierra Nevada surface. This result is at odds with the postulated "shallow subduction", or "flat slab" hypothesis, very often used to explain the sudden inland shift of magmatism in the western US during the Laramide orogeny, at the end of the Cretaceous (e.g., Dickinson 1981). This hypothesis predicts a significant decrease of the subducting slab dip, and accordingly the depth to the slab top beneath the western US Cordillera starting at 65 Ma, and continuing for possibly as many as 40 million years. More specifically, the slab top has been postulated to have passed as shallow as 35–60 km beneath the Sierra Nevada in Early Cenozoic times (Dumitru 1990), refrigerating the Sierra Nevada throughout the Cenozoic. Ague and Brandon (1996) have challenged this idea by proposing that the sudden demise of arc magmatism at Sierra Nevada latitudes can alternatively be explained by the "Baja-BC" hypothesis, which states that fragments of continental crust originally located to the west of the California batholiths (Sierra Nevada, Peninsular Ranges) were displaced northward for some 3000 to 4000 km along major strike-slip faults. Ague and Brandon presented evidence suggesting that the magmatic arc migrated northward, not eastward, therefore eliminating the need for a Laramide flat slab beneath much of the southwestern United States. The data presented here require that the refrigeration mechanism, if valid could not have involved a slab shallower than 130 km beneath the central Sierra at any time since the Mesozoic. The 130 km depth constrained from our data raises serious questions regarding the viability of the flat slab mechanism, at least under central California.

Contrasting post-batholith tectonics of the central and southern Sierra Nevada

The southernmost end of the Sierra Nevada batholith is exposed to igneous intrusion depths as high as 30 km, in the Tehachapi Mountains (Pickett and Saleeby 1993). Ensimatic metamorphic rocks of the Rand Schist tectonically underlie these deepest exposures of the batholith (Malin et al. 1995). The Rand Schist, as well as equivalent rocks found elsewhere in Southern California (Orocopia, Pelona Schists), has an oceanic derivation (Jacobsen et al. 1996). These relations show that the integrity of the Sierra Nevada batholith has not been maintained in its southernmost end. One can assume that the southernmost Sierra also had a similarly thick mafic–ultramafic "keel", as the central Sierra Nevada did. Therefore it is reasonable to infer that very shallow subduction has removed the batholith root at its southernmost end. The timing of the underthrusting of the Rand Schist is constrained by field relations and geochronologic data to be 80–86 million years (Silver and Nourse 1986). This period corresponds to a major cooling and uplift period throughout the entire Mojave area to the south and south east of the Sierra Nevada (Henry and Dokka 1992).

The observations presented above suggest a major difference between the post batholith tectonic behavior of the lithosphere in the central versus the southern(most) Sierra Nevada. Whereas the main part of the batholith retained its crustal wealth throughout the Cenozoic (at least until Mid-Miocene) and maintained elevations above sea level, the southern end of the batholith, which is representative for the Mojave region, has been the site of shallow subduction, lost its lower crust and was submerged below sea level during the Miocene (Nilsen and Clarke 1975). The southern versus central Sierra post-batholithic tectonic difference may be analogous to the modern Andes, where the central segment of the magmatic arc is underlain by a shallowly subducting slab, while the northern and southern Andes by steeper segments of the slab (Isacks 1988, and references therein).

Concluding remarks

The geochronologic results presented here confirm that the Sm-Nd mineral isochron method of dating garnet-rich rocks can successfully be applied to xenoliths to yield the timing of the peak thermal conditions. The Rb-Sr mineral isochron method applied on the same minerals is not nearly as reliable. We show that deep seated olivine-free xenoliths which equilibrated at pressures as high as 3.3 GPa locked-in Sm-Nd mineral ages consistent with a batholith residual origin. The existence of an

unusually cold lithosphere beneath the Sierra Nevada following the cessation of the batholith (Dumitru 1990) and the elevated blocking temperatures of the Sm-Nd and Rb-Sr systems in garnet-pyroxenes rocks with large grain size (Coghlan 1990; Metzger et al. 1992) have prevented most deep samples analyzed in this study from reequilibrating by diffusion during the Cenozoic.

The data presented in this paper provide a more complete view of the vertical dimension of a large Cordilleran batholith. The Sierra Nevada batholith consists of at least a 2/1 ratio of mafic–ultramafic to granitic material. We have shown that the central parts of the batholith were underlain by at least a ~70 km thick sequence of olivine-free mafic–ultramafic cumulate rocks in granulite and eclogite facies, probably mixed with peridotites at great depths. These rocks have isotopically equilibrated between ~80–120 Ma, coincident with the most prolific period of magmatism in the SNB. The isochron intercepts for the Sr and Nd isotopic ratios of the xenoliths presented here as well as age-corrected whole-rock analyses of similar xenoliths (Mukhopadhyay 1989) are identical to the isotopic ratios of the surface batholith in the vicinity of the xenolith-bearing Miocene pipes. The xenoliths are clearly batholith-related rocks. Textural and chemical (Ducea et al. 1997) arguments suggest these rocks are either cumulates from large lower crustal magma chambers, restites of large scale crustal melting, or both. We hypothesize that at least a 100 km thick lithospheric section beneath the Sierra Nevada batholith was strongly affected by the Mesozoic magmatism, homogenized isotopically and reset thermochronologically. Large scale magmatism efficiently segregated a high silica upper 30 km or so of crust from residual/cumulate rocks in the deeper parts of the crust and mantle.

The late Mesozoic to Miocene central Sierra Nevada lithosphere is constrained by xenolith data to be at least ~130 km thick. The thick batholithic lithosphere beneath the central Sierra Nevada raises serious questions as to whether a flat slab has ever existed beneath central California. On the other hand it points out a major tectonic difference between the post-batholith behavior of the central and southernmost Sierra Nevada: the southernmost Sierra and the Mojave regions were truncated at depth by an oceanic-like slab as shallow as 30 km at the end of the Cretaceous.

Acknowledgments. This research was funded through the NSF grant EAR-9526859 (to J. Saleeby). M. Ducea acknowledges grant #5810-96 from the Geological Society of America. Earlier versions of this manuscript were reviewed by Roberta Rudnick, Lang Farmer, John Eiler, James Chen, and Julia Goreva. Journal reviews by Jay Ague and Drew Coleman have significantly improved the quality of the manuscript. This is California Institute of Technology Division of Geological and Planetary Sciences contribution # 8483.

References

Ague JJ (1997) Thermodynamic calculation of emplacement pressures for batholithic rocks, California: implications for the aluminium-in-hornblende barometer. Geology 25: 563–566

Ague JJ, Brandon MT (1996) Regional tilt of the Mt. Stuart batholith, Washington, determined using Al-in-hornblende barometry; implications for northward translation of Baja British Columbia. Geol Soc Am Bull 108: 471–488

Ague JJ, Brimhall GH (1988) Magmatic arc asymmetry and distribution of anomalous plutonic belts in the batholiths of California; effects of assimilation, crustal thickness and depth of crystallization. Geol Soc Am Bull 100: 912–927

Ashworth JR (1985) Migmatites. Blackie, Glasgow, p 302

Bateman PC (1983) A summary of critical relationships in the central part of the Sierra Nevada batholith, California, U.S.A.. In: Roddick JA (ed) *Circum-Pacific plutonic terranes*. Geol Soc Am Mem 159, pp 241–254

Bateman PC, Dodge FCW (1970) Variations of major chemical constituents across the central Sierra Nevada batholith. Geol Soc Am Bull 81: 409–420

Bateman PC Eaton JP (1967) Sierra Nevada batholith. Science 158: 1407–1417

Burton KW, Kohn MJ, Cohen AS, O'Nions RK (1995) The relative diffusion of Pb, Nd, Sr, and O in garnet. Earth. Planet Sci Lett 133: 199–211

Carswell DA (1990) Eclogite facies rocks. Chapman and Hall, New York, NY

Chen JH, Tilton GR (1991) Applications of lead and strontium isotopic relationships to the petrogenesis of granitoid rocks, central Sierra Nevada batholith, California, Geol Soc Am Bull 103: 439–447

Chen JH, Moore JG (1982) Uranium-lead isotopic ages from the Sierra Nevada batholith, California. J Geophys Res 87: 4761–4784

Clemens, JD (1988) The granulite-granite connection. In: Vielzeuf D, Vidal P (eds) *Granulites and crustal evolution*. Ser C, 311, Kluwer Acad, Norwell, MA, pp 25–37

Coghlan R (1990) Studies in diffusional transport: grain boundary transport of oxygen in feldspar, diffusion of O, Sr, and REEs in garnet and thermal histories of granitic intrusions in south-central Maine using oxygen isotopes, PhD thesis, Providence, Rhode Island, Brown Univ

Coleman D, Glazner A (1998) The Sierra crest magmatic event; rapid formation of juvenile crust during the Late Cretaceous in California. In: Ernst, WG & Nelson CA (eds) Integrated Earth and Environmental Evolution of the Southwestern United States, pp 253–272, Bellwether Publishing Ltd., Columbia, MD

Coleman D, Frost T, Glazner A (1992) Evidence from the Lamarck Granodiorite for rapid Late Cretaceous crust formation in California. Science 258: 1924–1926

Coleman R, Lee D, Beatty J, Brannock W (1965) Eclogites and eclogites; their differences and similarities. Geol Soc Am Bull 76: 483–508

Coward MP, et al (1986) Collision tectonics in NW Himalayas. In: Coward MP, Ries AC (eds) *Collision tectonics*. Geol Soc Spec Publ 19, pp 203–219

DePaolo (1981) A neodynium and strontium study of the Mesozoic calc-alkaline granitic batholiths of the Sierra Nevada and Peninsular Ranges. J Geophys Res 86: 10470–10488

Dickinson W (1981) Plate tectonics and the continental margin of California. In: Ernst WG (ed) *The geotectonic development of California*. Prentice-Hall, Englewood Cliffs, NJ, pp 1–28

Dodge FCW, Bateman PC (1988) Nature and origin of the root of the Sierra Nevada. Am J Sci 288A: 341–357

Dodge FCW, Calk LC, Kistler RW (1986) Lower crustal xenoliths, Chinese Peak lava flow, Central Sierra Nevada. J Petrol 27: 1277–1304

Dodge FCW, Lockwood JP, Calk LC (1988) Fragments of the mantle and crust beneath the Sierra Nevada batholith: xenoliths in a volcanic pipe near Big Creek, California. Geol Soc Am Bull 100: 938–947

Dodge FCW, Millard HT Jr, Elsheimer HN (1982) Compositional variations and abundances of selected elements in granitoid rocks and constituent minerals, central Sierra Nevada batholith, California. US Geol Surv Prof Pap 1248

Dodson MH (1973) Closure temperature in cooling geochronological and petrological systems. Contrib Mineral Petrol 40: 259–274

Domenick MA, Kistler RW, Dodge FCW, Tatsumoto M (1983) Nd and Sr study of crustal and mantle inclusions from the Sierra Nevada and implications for batholith petrogenesis. Geol Soc Am Bull 94: 713–719

Ducea MN, Saleeby JB (1996a) Buoyancy sources for a large unrooted mountain range, the Sierra Nevada, California: evidence from xenolith thermobarometry. J Geophys Res 101: 8229–8241

Ducea MN, Saleeby JB (1996b) Rb-Sr and Sm-Nd mineral ages of some Sierra Nevada xenoliths; implications for crustal growth and thermal evolution. EOS Trans Am Geophys Union 77: 780

Ducea MN, Saleeby JB, Taylor HP Jr (1997) Constraints on the petrogenesis of the Sierra Nevada batholith from TP, geochronological, chemical and isotopic data on lower clustal xenoliths, Geol. Soc. Am Abstr. With Programs, V. 29, p 68

Dumitru TA (1990) Subnormal Cenozoic geothermal gradients in the extinct Sierra Nevada magmatic arc: consequences of Laramide and post-Laramide shallow subduction. J Geophys Res 95: 4925–4941

Ellis DJ, Green EH (1979) An experimental study of the effect of Ca upon garnet-clinopyroxene Fe-Mg exchange equilibria. Contrib Mineral Petrol 66: 13–22

Everden JF, Kistler RW (1970) Chronology of emplacement of Mesozoic batholithic complexes in California and western Nevada. US Geol Surv Prof Pap 623: 1–42

Fliedner M, Ruppert S (1996) 3-dimensional crustal structure of the Southern Sierra Nevada from seismic fan profiles and gravity modeling. Geology 24: 367–370

Green DH, Ringwood AE (1967) An experimental investigation of the gabbro to eclogite transformation and its petrological applications. Geochim Cosmochim Acta 31: 767–833

Gromet P, Silver LT (1987) REE variations across the Peninsular Ranges Batholith: I Implications for batholithic petrogenesis and crustal growth in magmatic arcs. J Petrol 28: 75–125

Hamilton W, Myers WB (1966) The nature of batholiths. US Geol Surv Prof Pap 554C

Harrison TM, Wood BJ (1980) An experimental investigation of the partitioning of REE between garnet and liquid with reference to the role of defect equilibrium. Contrib Mineral Petrol 72: 145–155

Harley SL (1984) An experimental study of the partitioning of Fe and Mg between garnet and orthopyroxene. Contrib Mineral Petrol 86: 359–373

Harley SL, Green DH (1982) Garnet-orthopyroxene barometry for granulites and peridotites. Nature 300: 697–701

Henry DJ, Dokka RK (1992) Metamorphic evolution of exhumed middle to lower crustal rocks in the Mojave Extensional Belt, southern California, USA. J Metamorphic Geol 10: 347–364

Hunter RH (1986) Textural equilibrium in layered igneous rocks. In: Parsons I (ed) *Origin of igneous layering*. (NATO ASI Ser C, 196) Kluwer Acad Norwell, MA, pp 473–505

Isacks BL (1988) Uplift of the central Andean Plateau and bending of the Bolivian orocline. J Geophys Res 93: 3211–3231

Jacobsen CE, Oyarzabal FR, Haxel GB (1996) Subduction and exhumation of the Pelona-Orocopia-Rand schists, southern California. Geology 24: 547–550

Jagoutz E (1988) Nd and Sr systematics in an eclogite xenolith from Tanzania: evidence for frozen mineral equilibria in the continental lithosphere. Geochim Cosmochim Acta 52: 1285–1293

Kay RW, Kay SM (1993) Delamination and delamination magmatism, Tectonophysics 219: 177–189

Kistler RW, Peterman Z (1973) Variations in Sr, Rb, K, Na and initial $^{87}Sr/^{86}Sr$ in Mesozoic granitic rocks and intruded wall rocks in central California. Geol Soc Am Bull 84: 3489–3512

Kistler RW, Peterman Z (1978) Reconstruction of crustal blocks of California on the basis of initial Sr isotopic compositions of Mesozoic granitic rocks. US Geol Surv Prof Pap 1071

Klein EM, Langmuir CH (1987) Global correlations of ocean ridge basalt chemistry with axial depth and crustal thickness. J Geophys Res 92: 8089–8115

Lachenbruch AH (1968) Preliminary geothermal model of the Sierra Nevada. J Geophys Res 73: 6977–6989

Ludwig K (1991) ISOPLOT, a plotting and regression program for radiogenic isotope data. US Geol Surv Open-file Rep 91–445

Malin PE, Goodman ED, Henyey TL, Li YG, Okaya DA, Saleeby JB (1995) Significance of seismic reflections beneath a titled exposure of deep continental crust, Tehachapi Mountains, California. J Geophys Res 100: 2069–2087

Manning CE, Bohlen SR (1991) The reaction titanite + kyanite = rutile + anorthite and titanite-rutile barometry in eclogites. Contrib Mineral Petrol 109: 1–9

Masi U, O'Neill JR, Kistler RW (1981) Stable isotope systematics in Mesozoic granites of central and northern California and southwestern Oregon. Contrib Mineral Petrol 76: 116–126

Metzger K, Essene EJ, Halliday AN (1992) Closure temperatures of the Sm-Nd system in metamorphic garnets. Earth Planet Sci Lett 113: 397–409

Moore JG, Dodge FCW (1980) Late Cenozoic volcanic rocks of the Southern Sierra Nevada, California. I. Geology and petrology: summary. Geol Soc Am Bull 91: 515–518

Mukhopadhyay B (1991) Garnet breakdown in some deep seated garnetiferous xenoliths from the central Sierra Nevada: petrologic and tectonic implications. Lithos 27: 59–78

Mukhopadhyay B (1989) Petrology and geochemistry of mafic and ultramafic xenoliths from the Sierra Nevada batholith. 1. PhD diss, Univ Texas at Dallas

Mukhopadyay B, Manton WI (1994) Upper mantle fragments from beneath the Sierra Nevada batholith: partial fusion, fractional crystallization and metasomatism in a subduction-enriched ancient lithosphere. J Petrol 35: 1418–1450

Newton RC, Perkins D (1982) Thermodynamic calibrations of geobarometers based on the assemblages garnet-plagioclase-orthopyroxene (clinopyroxene)-quartz. Am Mineral 67: 203–222

Nilsen TH, Clarke SH (1975) Sedimentation and tectonics in the early Tertiary continental borderland of central California US Geol Surv Prof Pap 925

Pattison DRM, Newton RC (1989) Reversed experimental calibration of the garnet-clinopyroxene Fe-Mg exchange thermometer. Contrib Mineral Petrol 101: 87–103

Pickett DA, Saleeby JB (1993) Thermobarometric constraints on the depth of exposure and conditions of plutonism and metamorphism at deep levels of the Sierra Nevada batholith, Tehachapi Mountains, California. J Geophys Res 98: 609–629

Pickett DA, Saleeby JB (1994) Nd, Sr, and Pb isotopic characteristics of Cretaceous intrusive rocks from deep levels of the Sierra Nevada batholith, Tehachapi Mountains, California. Contrib Mineral Petrol 118: 198–205

Pitcher WS (1993) The nature and origin of granite. Blackie Acad and Prof, London

Rapp RP, Watson EB (1995) Dehydration melting of metabasalt at 8–32 kbar: implications for continental growth and crust-mantle recycling. J. Petrol 36: 891–931

Rudnick RL (1992) Xenoliths: samples of the lower continental crust. In: Fountain DM, Arculus R, Kay RW (eds) *Lower continental crust*. (Developments in geotectonics, 23) pp 269–317, Elsevier, New York

Saleeby JB (1990) Progress in tectonic and petrogenetic studies in an exposed cross-section of young (c. 100 Ma) continental crust, southern Sierra Nevada, California. In: Salisbury MH, Fountain DM (eds) *Exposed crustal sections of the continental crust*. Kluwer Acad, Norwell, MA pp 137–158

Saleeby JB, Sams DB, Kistler RW (1987) U/Pb zircon, strontium, and oxygen isotopic and geochronological study of the southernmost Sierra Nevada batholith, California. J Geophys Res 92: 10443–10466

Silver LT, Nourse JA (1986) The Rand Mountains thrust complex in comparison with the Vincent thrust-Pelona schist relation-

ship, southern California (abstract). Geol Soc Am Abstr Program 18: 185
Sneeringer M, Hart SR, Shimizu N (1984) Strontium and samarium diffusion in diopside. Geochim Cosmochim Acta 48: 1589–1608
Wendlandt E, DePaolo DJ, Baldridge WS (1996) Thermal history of Colorado Plateau lithosphere from Sm-Nd mineral geochronology on xenoliths. Geol Soc Am Bull 108: 757–767
Wendt I, Carl C (1991) The statistical distribution of the mean squared weighted deviation. Chem Geol 86: 275–285
Wernicke B, et al. (1996) Origin of high mountains on continents: the Southern Sierra Nevada. Science 271: 190–193
Wolf MB, Wyllie PJ (1993) Garnet growth during amphibolite anatexis: implications for a garnetiferous restite. J Geol 101: 357–373
Wyllie PJ (1984) Constraints imposed by experimental petrology on possible and impossible magma sources and products. Philos Trans R Soc London A310: 439–456
York D (1969) Least-squares fitting of a straight line with correlated errors. Earth Sci Planet Lett 5: 320–324